

# Probing thermal conductivity of interphase in epoxy alumina nanocomposites

Manohar Singh  and Jeewan Chandra Pandey 

Polymers and Polymer Composites  
Volume 30: 1–11  
© The Author(s) 2022



Article reuse guidelines:  
[sagepub.com/journals-permissions](https://sagepub.com/journals-permissions)  
DOI: 10.1177/09673911221077489  
[journals.sagepub.com/home/ppc](https://journals.sagepub.com/home/ppc)



## Abstract

The objective of this research is to determine the thermal conductivity of the interphase in epoxy alumina nanocomposites. First, TPS 500 measures the thermal conductivity of epoxy alumina nanocomposite samples. Following that, a numerical model based on the finite element method was developed to estimate the effective thermal conductivity of epoxy alumina nanocomposites over a range of assumed interphase thermal conductivity values. Finally, an algorithm is devised to extract the interphase's thermal conductivity by combining simulation and experiment results. Interphase was found to have significantly higher thermal conductivity than the base polymer. A comprehensive analysis is presented to shed light on the observed increase in interphase thermal conductivity. The findings of this study will be critical for further investigation of heat transfer in epoxy alumina nanocomposites via modeling and simulation studies.

## Keywords

nanocomposites, thermal conductivity, electrical insulation, interphase

Received 17 May 2021; accepted 7 January 2022

## Introduction

Electrical insulation forms the backbone of all electrical power networks. The life of electrical insulation is determined by its aging characteristics under various operating stresses (i.e., electrical, mechanical, thermal, and ambient). Failure data reveals that the majority of electrical insulation failures occur due to thermal stress.<sup>1</sup> Thermal stress originates in electrical equipment due to heat produced by different losses (ohmic, magnetic, and dielectric). The temperature rise caused by trapped heat gradually decreases the dielectric material's performance and eventually results in premature failure. On the other hand, increased thermal conductivity enables more efficient heat transfer, extending the life expectancy of electrical equipment.

Polymeric insulating materials are attractive to electrical insulation designers due to their low electrical conductivity, high dielectric strength, high strength-to-weight ratio, and hydrophobic properties. Despite many fascinating features, low thermal conductivity prevents their extensive usage in electrical power devices and systems. Low electrical conductivity and high thermal conductivity have become increasingly desirable for insulating materials operating at elevated voltage levels. In recent years, polymer nanocomposites (PNCs) have gained prominence as potential solutions for addressing these two seemingly contradictory requirements.<sup>2–5</sup> Polymer nanocomposites are a class of materials in which nanometer-sized particles are uniformly dispersed in a host polymer to improve its electrical, mechanical, and thermal properties.<sup>6–10</sup> Interfacial interaction becomes a dominant parameter to regulate the properties of nanocomposites due to the enormous specific surface area of nanoparticles. A substantial body of literature indicates that filler matrix interaction in PNCs constitutes a new phase called interphase. Interphase appears to be crucial in strengthening the attributes of PNCs. On the other hand, the interphase characteristics are unknown and are likely to differ significantly from the filler and base polymer. The understanding of the physicochemical interactions at interfaces has advanced significantly in recent years.<sup>11–16</sup> Apart from comprehending the physicochemical interaction of filler and matrix, quantifying the interphase's size and material properties are crucial to investigating nanocomposites through modeling and simulation studies.

Due to its favorable electrical insulating properties, epoxy resin (a thermoset polymer) is commonly used in various applications, including power transformers, post insulators, rotating machines, GIS spacers, bushings, and printed circuits boards. Micro-sized alumina fillers possess good mechanical and thermal properties, and they are commonly utilized to

Department of Electrical Engineering, Indian Institute of Technology (BHU), Varanasi, India

## Corresponding author:

Jeewan Chandra Pandey, Department of Electrical Engineering, Indian Institute of Technology (BHU), Room No 78, ASN Bose Hostel Near Hyderabad gate, Varanasi 221005, India.

Email: [jcpandey.eee@itbhu.ac.in](mailto:jcpandey.eee@itbhu.ac.in)

augment the structural strength and discharge resistance of epoxy resins. The limited interfacial region, or interphase, makes it easier to predict the material properties of micro-composites. On the other hand, nanocomposites have a high fraction of interphase. Therefore, to determine the influence of nanofiller inclusion on the thermal characteristics of epoxy resin, characterization of the interphase is necessary. Nevertheless, there is indeed a paucity of research on this subject. Prior work by the authors effectively delineated interphase in terms of its size and dielectric characteristics.<sup>11,17</sup> Table 1 presents numerical values for key constituents' dielectric properties derived from previous studies.

This research extends previous work by probing the thermal conductivity of the interphase in epoxy alumina nanocomposites. A finite element method (FEM) based numerical model has been developed to estimate the effective thermal conductivity of nanocomposites. The TPS 500 instrument is used to measure the thermal conductivity of synthesized samples. Finally, an algorithm is devised to estimate the interphase's thermal conductivity using simulation and experiment results.

## Materials

Epoxy resin (DGEBA) supplied by Huntsman is used as a base material. Spherical aluminum oxide (alumina) nanoparticles with an average size of 50 nm were employed as nanofillers. Sigma Aldrich's 3-glycidoxypropyl trimethoxysilane (GPS) was employed to surface functionalize alumina nanoparticles. Triethylenetetramine, supplied by Huntsman, was used as the curing agent.

### Preparation of the samples

The following specimens were synthesized for this study:

1. Pure epoxy samples.
2. Nanocomposites samples (with nano alumina concentrations of 1 and 2 vol.%).

Pure epoxy samples were synthesized by gently mixing the 10% hardener with neat epoxy resin. The solution is then degassed to get rid of any trapped gas bubbles. The degassed solution was then poured into the mold and allowed to cure for 24 h at room temperature. In addition, 12 h of post-curing at 100°C were completed. Finally, 15x15x15 mm cubic samples were fabricated to meet the dimensional specifications of the measuring instrument (TPS 500).

To fabricate nanocomposite samples, a procedure similar to that described in Refs. 18 and 19 is adopted. The first step in this procedure is to prepare a solution made up of 95% ethanol and 5% distilled water. The pH of the solvent is brought up to 4.5 by adding acetic acid. While the solution is sonicated, a predetermined amount of 3-glycidoxypropyl trimethoxy silane (GPS) is gently injected. The silane must be allowed to hydrolyze entirely after 30 min of sonication. Next, untreated alumina nanoparticles are introduced to the hydrolyzed GPS solution at regular intervals to ensure homogeneous dispersion and coating of the nanoparticles. After that, the mixture is sonicated for an additional hour. The solvent is then evaporated, resulting in surface-functionalized nanoparticles. Finally, employing Fourier transform infrared spectroscopy (FTIR), the surface functionalization of nanoparticles is confirmed.<sup>11</sup> To prepare samples, a predetermined amount of surface-functionalized alumina nanoparticles was added to ethanol and dispersed uniformly for 60 min using ultrasonication. Next, a predetermined amount of epoxy was added to the ultrasonicated solution and thoroughly stirred with a magnetic stirrer. Following the removal of the ethanol, the nanocomposite samples were prepared in the same manner as the pure epoxy samples. Figure 1 depicts typical images of synthesized epoxy and nanocomposite samples (with a filler content of 1 vol.%). A flow diagram illustrating the synthesis of nanocomposite samples is shown in Figure 2.

### Scanning electron microscopy

Scanning electron microscopy (SEM) was used to examine the morphology of the samples. Figure 3 shows typical micrographs of pure epoxy and nanocomposites (at a filler content of 1 vol. %) samples. There is no visible particle agglomeration, indicating that the particles are evenly distributed throughout the host polymer.

**Table 1.** Dielectric properties of constituent phases in epoxy alumina nanocomposites.

Substance	Dielectric constant	DC conductivity
Host polymer (epoxy resin)	4.00	$1.98 \times 10^{-14}$ (S/m)
Nanofiller (Alumina)	10.0	$1.00 \times 10^{-12}$ (S/m)
Interphase	3.73	$0.96 \times 10^{-14}$ (S/m)

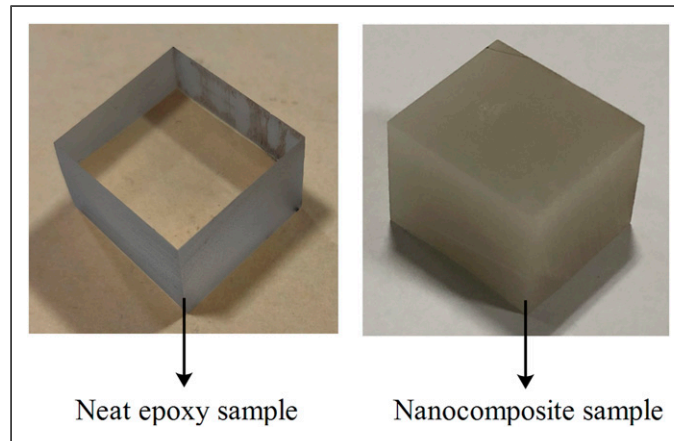


**Figure 1.** Synthesized neat epoxy and nanocomposite samples.

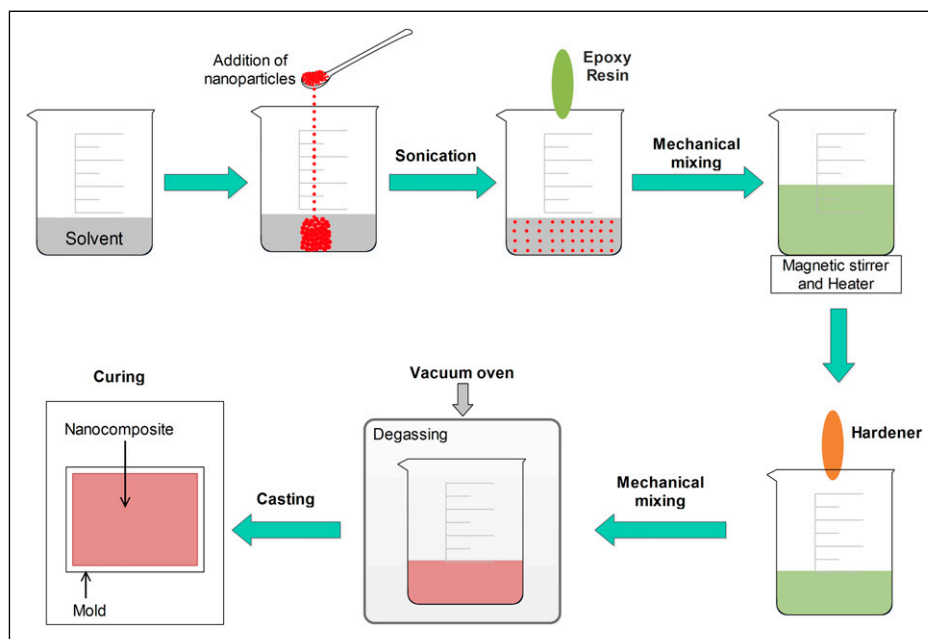


**Figure 2.** Flow diagram for the synthesis of the nanocomposites.

### Thermal conductivity measurement

The standard test technique recommended by ISO 22007-2:2008 was followed while measuring thermal conductivity using a TPS 500 instrument. Thermal conductivity measurements are carried out by sandwiching the TPS 500 sensor between two segments of a sample, as illustrated in Figure 4. A total of five samples from each specimen were randomly selected and tested for thermal conductivity. Table 2 shows the average thermal conductivity value of each specimen.

### Numerical modeling

A numerical model implemented in COMSOL Multiphysics is used to estimate the effective thermal conductivity of nanocomposites. The following subsections discuss numerical modeling in greater detail.

#### Pre-processing

First, a unit cell with a size of  $1 \mu\text{m} \times 1 \mu\text{m} \times 1 \mu\text{m}$  is constructed, which comprises 1 vol.% alumina particles of size 50 nm. One hundred fifty-three (153) filler particles are randomly distributed within the unit cell of the numerical model to ensure the filler content in the numerical model is identical to the filler content of the synthesized samples. Each nanoparticle is surrounded by interphase with a specified thickness determined by previous studies.<sup>17</sup> Apart from filler and interphase, neat epoxy occupies the remainder of the volume in the unit cell. Figure 5 illustrates a unit cell composed of three material domains (i.e., neat epoxy, alumina nanofillers, and interphase). The application builder tool of COMSOL Multiphysics in conjunction with the JAVA script's random function is used to build the numerical model, and periodic boundary conditions are appropriately applied. Based on the

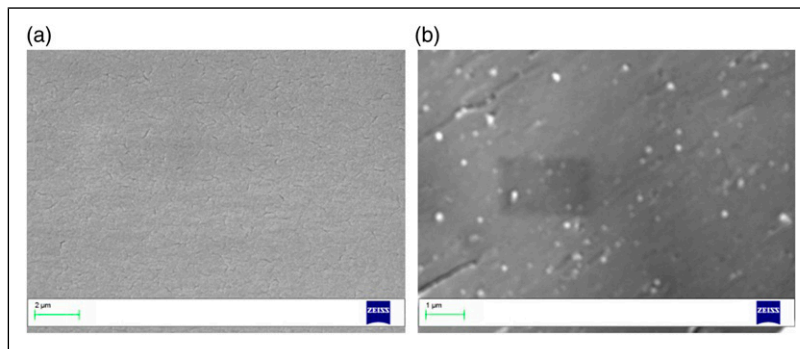


**Figure 3.** Scanning electron microscopy micrographs: (a) neat epoxy (b) epoxy alumina nanocomposites.

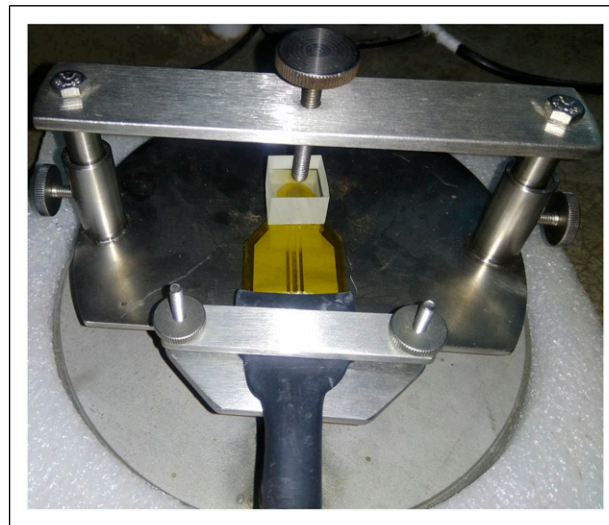


**Figure 4.** TPS 500 sensor sandwiched between samples.

**Table 2.** Measured thermal conductivity values of different specimen.

Specimen	Thermal conductivity (W/K.m)
Neat epoxy sample	$0.160 \pm 1\%$
Nanocomposites sample (with filler content of 1 vol.%)	$0.174 \pm 1\%$
Nanocomposites sample (with filler content of 2 vol.%)	$0.192 \pm 1\%$

experimental data shown in Table 2, epoxy resin is assigned a thermal conductivity of 0.16 W/K.m. According to the manufacturer's specification, alumina nanoparticles have a thermal conductivity of 30 W/K.m. The analysis was carried out using the AC/DC module and heat transfer module of COMSOL Multiphysics. The electric field in the dielectric material is computed by solving the Laplace equation and the continuity equation (Maxwell's equation for conservation of charge). It is required to first compute the conduction losses in the dielectric materials. The thermal solver then estimates the temperature distribution based on the conduction losses that have occurred. The unit cell's outer boundary is kept at room temperature (i.e., 293°C).

The effective thermal conductivity of nanocomposites is estimated using equation (1) shown below

$$q = k.TG \quad (1)$$

where  $\langle q \rangle$  represents the average heat flux magnitude over the volume of the cube,  $k$  denotes the effective thermal conductivity, and  $\langle TG \rangle$  represents the temperature gradient. Figure 6(a) and Figure 6(b) illustrate typical plots of the heat flux and temperature gradient, respectively.

### Estimating thermal conductivity of interphase

A bisection method-based algorithm is utilized to evaluate the thermal conductivity of the interphase. The steps to implement the proposed algorithm are described in detail in the following section:

Step 1-Record experimental thermal conductivity values for pure epoxy and nanocomposites.

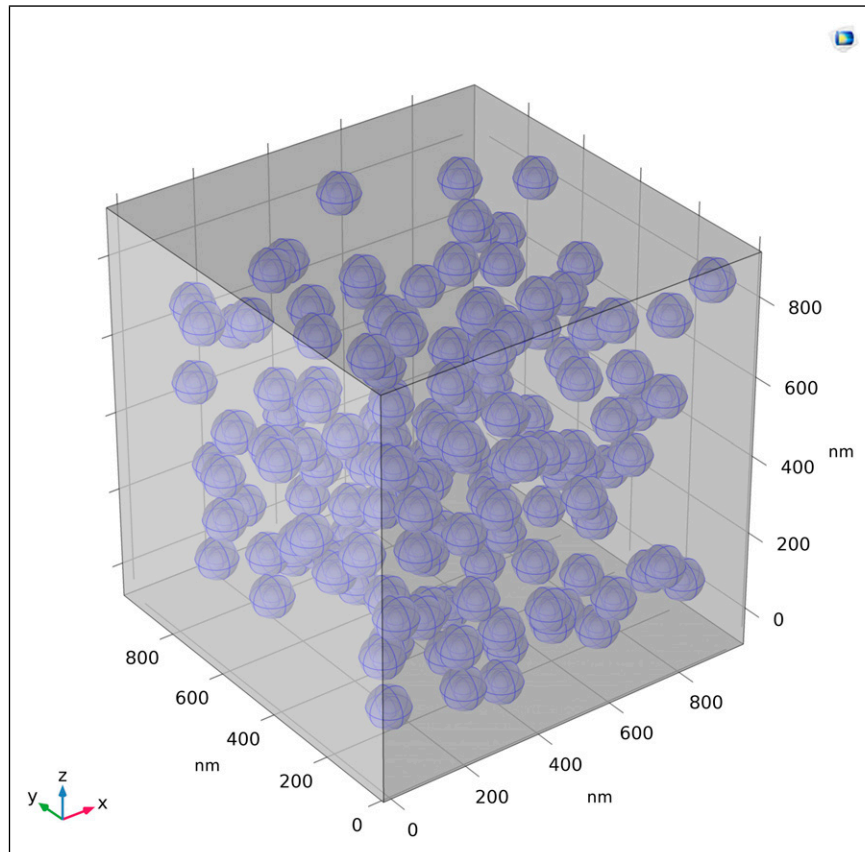


**Figure 5.** Randomly distributed nanoparticles in the epoxy matrix.

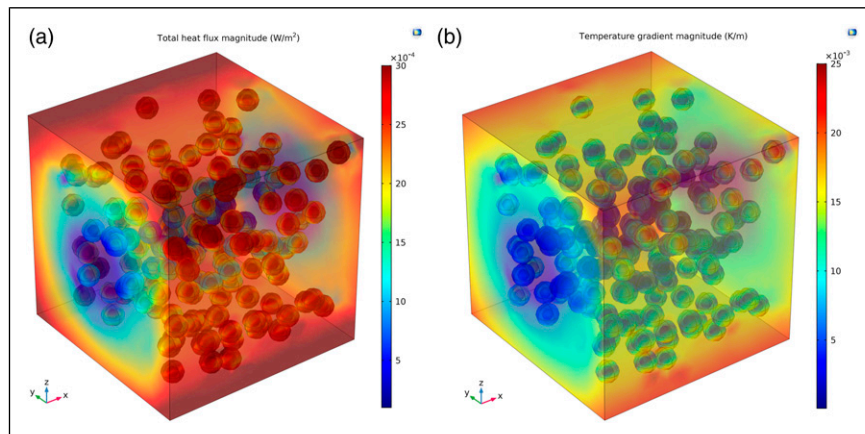


**Figure 6.** (a) Heat flux magnitude inside the model, (b) Temperature gradient magnitude inside the model.

Step 2: Import the model created in COMSOL Multiphysics. Assign material properties, describe the model's physics and apply appropriate boundary conditions.

Step 3-Set the simulated thermal conductivity of the nanocomposite to zero as an initial trial value. Specify a convergence tolerance value of 0.001. Assign a value of 0 as the initial mean, a value of 30 as the up bound, and a value of 0.001 as the low bound.

Step 4-Compare the measured thermal conductivity of nanocomposites to that computed using a numerical model. If this difference is greater than the convergence tolerance limit, go to the next step. If the difference is less than the convergence tolerance, store the interphase's thermal conductivity value and exit the program.

Step 5-Calculate the mean value of the up bound and low bound. Assign this mean value to interphase thermal conductivity.

Step 6-Calculate the total heat flux and temperature gradient using the numerical model. Determine the thermal conductivity of the nanocomposite using the total heat flux magnitude and temperature gradient. This nanocomposite thermal conductivity value should be stored.

Step 7: The computed value of the effective thermal conductivity of the nanocomposites is compared to the measured value. If the computed value exceeds the measured value, then assign the up bound value as the mean value. If the computed value is lower than the measured value, then a low bound is used as the mean.

Step 8-Return to step 4 and repeat until convergence is achieved.

The suggested method is also illustrated using the flow chart depicted in Figure 7 for clarity. Table 3 contains information on the variables used in the flow chart.

## Results and discussion

The thermal conductivity of alumina particles as specified by the manufacturer is 30 W/K.m, and the measured thermal conductivity of neat epoxy samples is 0.16 W/K.m. This shows that the epoxy resin possesses significantly lower thermal

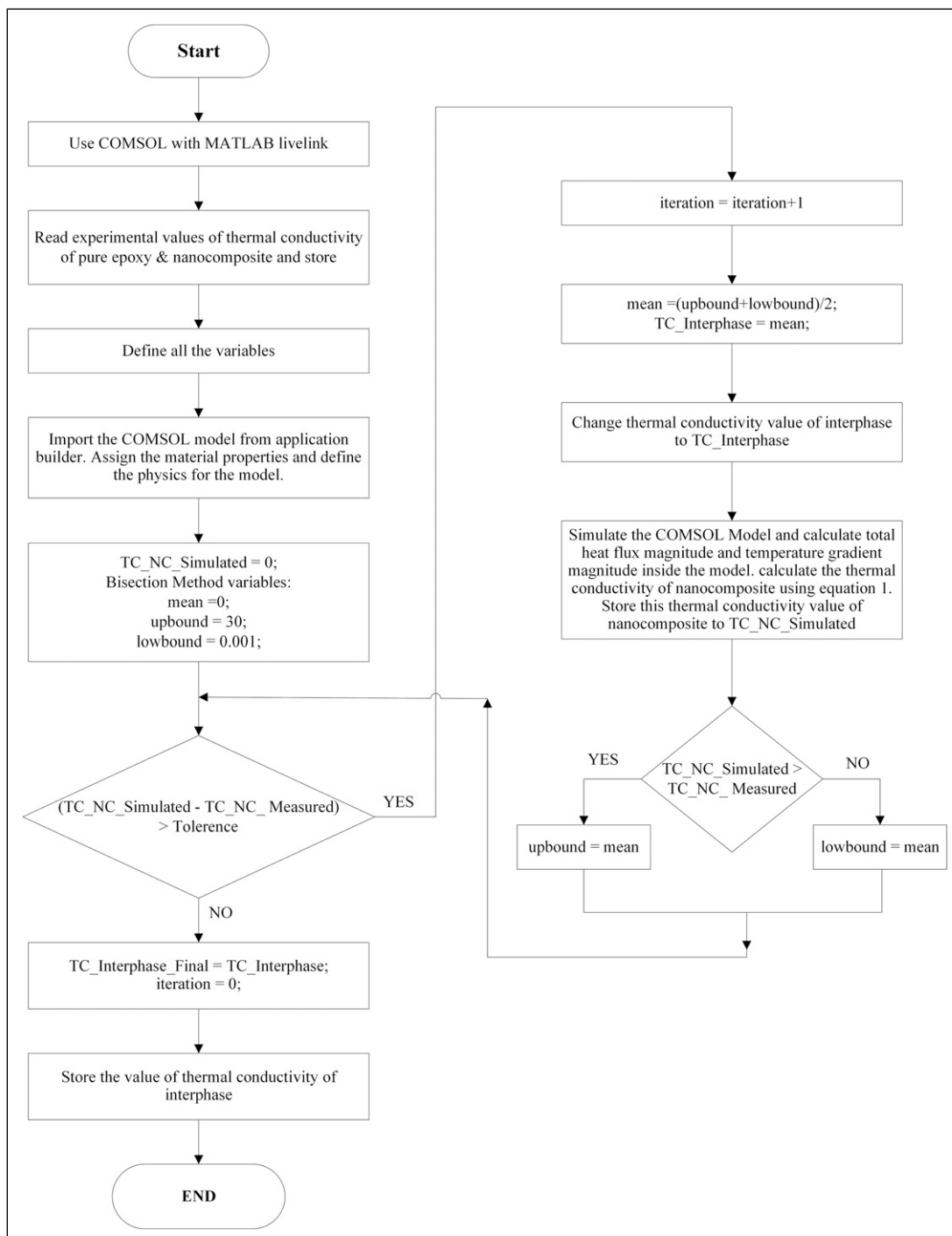
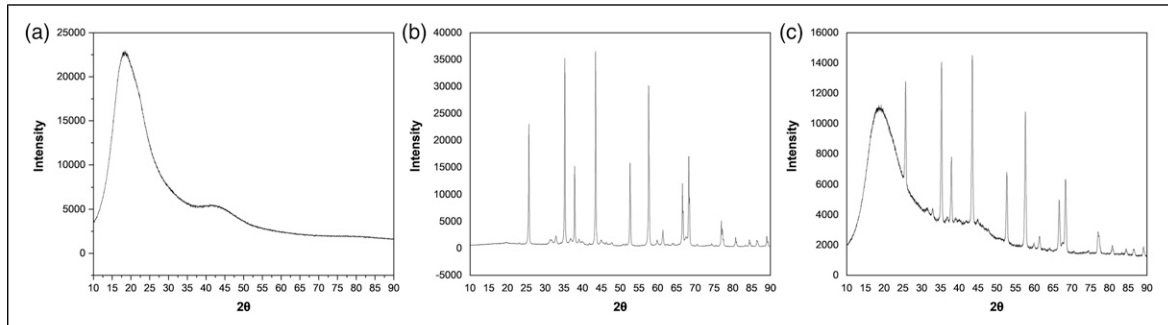
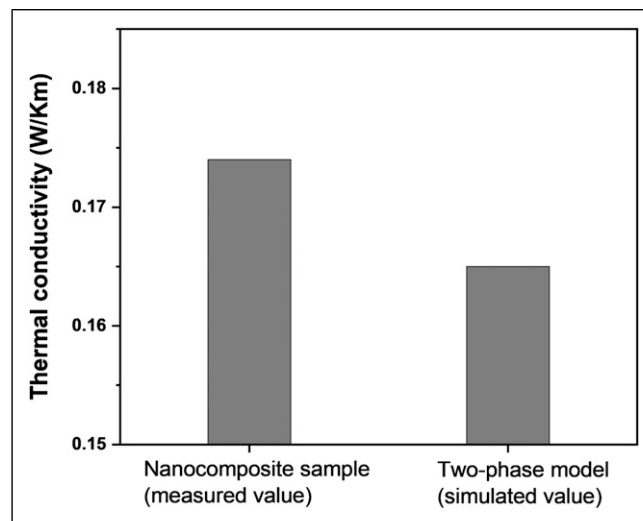


Figure 7. An illustration of the flowchart used to estimate the thermal conductivity of the interphase.

**Table 3.** List of variables used in the flowchart, along with their descriptions.

Variables	Details
TC_NC_Measured	The measured value of the thermal conductivity of nanocomposites
TC_NC_Simulated	Thermal conductivity of nanocomposite obtained through simulation
TC_Interphase	Thermal conductivity of interphase
TC_Interphase_Final	To store the final converged value of thermal conductivity of interphase
Up bound	A variable that represents the upper bound
Low bound	A variable that represents lower bound
Mean	A variable that represents the middle point of lower and upper bound

**Figure 8.** XRD graph of (a) Pure epoxy sample, (b) Alumina nanoparticles, (c) Epoxy alumina nanocomposite sample.**Figure 9.** Measured thermal conductivity of actual nanocomposites and simulated value (without considering interphase).

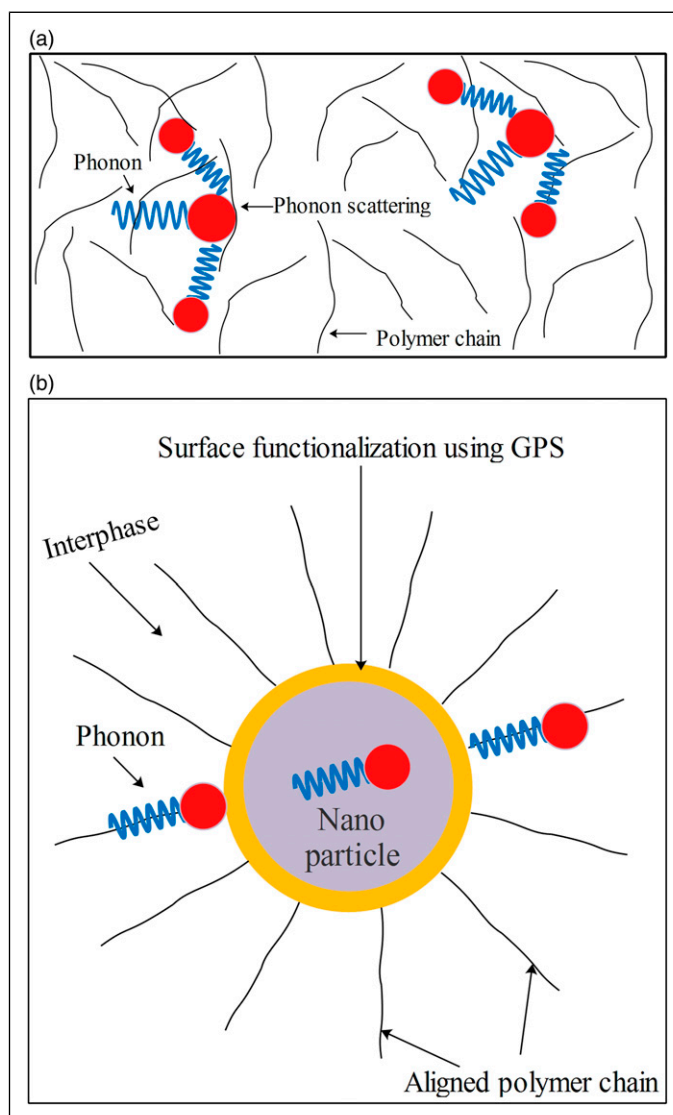
conductivity than alumina. Figures 8(a) and (b) show X-ray diffraction (XRD) spectra of epoxy and alumina nanoparticles, respectively.

The XRD pattern indicates the amorphous and crystalline nature of epoxy and alumina, respectively. One of the main reasons for the lower thermal conductivity of epoxy resin is its high degree of amorphousness. Besides being amorphous, epoxy resin exhibits low thermal conductivity due to its low atomic density and a higher mismatch in its molecular thermal vibrations.<sup>20</sup> Figure 8(c) depicts the XRD pattern of epoxy alumina nanocomposites, which clearly shows the presence of alumina particles in composite samples.

The effect of nanofiller inclusion on the thermal conductivity of epoxy is estimated using the numerical model described earlier. To begin with, the numerical model treats nanocomposites as a two-phase system. The computed thermal conductivity is then compared with the measured thermal conductivity. The bar chart in Figure 9 shows the measured and numerically estimated effective thermal conductivity of nanocomposite samples. The calculated thermal conductivity of nanocomposites is significantly lower than the measured value. Thus, considering a nanocomposite sample as a two-phase system is unacceptable, particularly when nanocomposites are synthesized using surface-treated nanoparticles. Pandey and Singh<sup>11</sup> presented a detailed analysis to demonstrate how the interaction of a surface-treated filler and a polymer matrix would

**Table 4.** Thermal conductivity of nanocomposites and their key constituents.

Substance	Thermal conductivity (W/K.m)
Nanocomposites (Epoxy alumina)	0.174
Host polymer (Epoxy resin)	0.160
Filler (Alumina)	30.00
Interphase	0.351

**Figure 10.** (a) Phonon scattering phenomena in a polymer, (b) Phonon transport phenomena through aligned polymers chains at the interface.

eventually form interphase. Furthermore, quantitative interphase analysis reveals that the interphase thickness in epoxy alumina nanocomposites can reach a few hundred nanometers.<sup>17</sup>

The preceding section's analysis estimates an interphase thermal conductivity of 0.351 W/K.m. Table 4 compares the thermal conductivity of nanocomposites and their constituent phases. The estimated thermal conductivity of the interphase is validated by comparing the numerically computed effective thermal conductivity and the measured thermal conductivity of nanocomposites with a 2 vol. % filler content. The effective thermal conductivity of nanocomposites is calculated numerically by assigning known material parameters (Table 4) to the various constituent phases. The computational model predicts an effective thermal conductivity of 0.191 W/K.m for nanocomposites with a filler concentrations of 2 vol. %, this closely matches the experimentally observed thermal conductivity in Table 2.

Furthermore, for a three-phase system, the effective thermal conductivity of composites should lie within the upper and lower Wiener bounds.<sup>21</sup> The upper and lower Wiener bounds are given by equation (2) and (3).



$$k_{upper} = \varphi_p \cdot k_p + \varphi_i \cdot k_i + (1 - \varphi_p - \varphi_i) \cdot k_m \quad (2)$$

$$k_{lower} = \left[ \frac{\varphi_p}{k_p} + \frac{\varphi_i}{k_i} + \frac{(1 - \varphi_p - \varphi_i)}{k_m} \right]^{-1} \quad (3)$$

where

- $k_{upper}$  - Upper Wiener bound
- $k_{lower}$  - Lower Wiener bound
- $\varphi_p$  - Volume fraction of filler particles
- $\varphi_i$  - Volume fraction of interphase
- $k_p$  - Thermal conductivity of filler particles
- $k_i$  - Thermal conductivity of interphase
- $k_m$  - Thermal conductivity of the matrix

For epoxy-based nanocomposites (formed with 1 vol.% of alumina),  $k_{upper}$  and  $k_{lower}$  are 0.471 W/K.m and 0.168 W/K.m, respectively. The effective thermal conductivity of epoxy alumina nanocomposites predicted using the numerical model is 0.174 W/K.m, and this value lies within the upper and lower Wiener bounds. Similarly, the effective thermal conductivity estimated by the proposed numerical model for nanocomposites (containing 2 vol.% of nano alumina) is within Wiener bounds.

Each of the studies outlined above verifies the numerical model's accuracy. The thermal conductivity of the interphase is calculated to be significantly greater than that of the neat polymer. The interphase's high thermal conductivity may be a result of the polymer chain's alignment at the filler matrix interfaces. Andritsch<sup>22</sup> proposed a polymer chain alignment model and explained how aligned chains might contribute to a nanocomposites sample's effective permittivity. Similarly, a few other researchers<sup>23-30</sup> have published on the impact of chain alignment on the thermal conductivity of polymers. Heat transfer in insulating polymers is thought to be primarily facilitated by phonon transport. The scattering of thermal energy carriers (phonons) is caused by the irregular crystal structures of polymers, as shown in Figure 10(a). Polymeric materials with increased phonon scattering have low thermal conductivity. Aligned polymer chains minimize interfacial resistance, thus facilitating phonon transport between filler and base epoxy and vice versa. The schematic in Figure 10(b) illustrates how aligned polymer chains at the interfaces can boost phonon transport, resulting in an increase in interphase thermal conductivity.

The bar chart in Figure 9 shows how interphase has a quantifiable impact on thermal conductivity estimates of nanocomposites. For example, the thermal conductivity of actual nanocomposites (made with surface-treated nanofillers) is 0.174. On the other hand, when nanocomposites are modeled as a two-phase system (i.e., without interphase), the effective thermal conductivity is found to be 0.164. This suggests that the interphase has a substantial impact on nanocomposites' thermal conductivity. In a similar line, interphase was seen to affect other dielectric characterizations (viz., dielectric strength, conductivity, and permittivity). The authors' earlier work<sup>11</sup> detailed systematic analysis of interphase formation in epoxy-based nanocomposites and its impact on dielectric properties.

## Conclusion

The thermal conductivity of epoxy alumina nanocomposites is investigated in this work. When epoxy alumina nanocomposites are treated as a two-phase system, numerically predicted thermal conductivity values do not concur with experimental values. Thus, one could argue that the interaction between the filler and the matrix results in the creation of interphase, which is particularly true when nanocomposites are formed using surface-treated nano alumina. This study makes the most significant contribution by developing a methodology for estimating the thermal conductivity of interphase using experimental data and numerical modeling. According to the proposed methodology, the thermal conductivity of the interphase in epoxy alumina nanocomposites is 0.351 W/K.m, which is significantly higher than that of pure epoxy. The increased thermal conductivity of the interphase may be due to the interaction of the filler matrix, which results in the alignment of polymer chains at the interfaces. Aligning polymer chains reduces phonon scattering, resulting in increased heat transfer efficiency. This research focuses exclusively on epoxy-based composites employing nano alumina fillers. At a low filler content (1 vol.% of nano alumina), the thermal conductivity of nanocomposites is seen to increase modestly for neat polymer. However, as evidenced in the published literature, boosting thermal conductivity at a high filler level necessitates a trade-off of dielectric properties. Thus, future work with various high thermal conductivity fillers should be undertaken in order to optimize the material's overall performance. From this vantage point, the current study points the way forward for future research on the electro-thermal analysis of polymer nanocomposites.

## Declaration of conflicting interests

The author(s) declared no potential conflicts of interest with respect to the research, authorship, and/or publication of this article.

## Funding

The author(s) received no financial support for the research, authorship, and/or publication of this article.

## ORCID iDs

Manohar Singh  <https://orcid.org/0000-0001-6137-1057>

Jeewan Chandra Pandey  <https://orcid.org/0000-0002-9871-7645>

## References

1. Stone GC, Culbert I, Boulter EA, et al. *Electrical Insulation for Rotating Machines: Design, Evaluation, Aging, Testing, and Repair Historical Development of Insulation Materials and Systems*. New Jersey, NJ: John Wiley & Sons, 2003.
2. Kashfipour MA, Mehra N and Zhu J. A review on the role of interface in mechanical, thermal, and electrical properties of polymer composites. *Adv Compos Hybrid Mater* 2018; 1(3): 415–439. DOI: [10.1007/s42114-018-0022-9](https://doi.org/10.1007/s42114-018-0022-9).
3. Wang X, Andritsch T, Chen G, et al. The role of the filler surface chemistry on the dielectric and thermal properties of polypropylene aluminium nitride nanocomposites. *IEEE Trans Dielectr Electr Insul* 2019; 26(3): 1009–1017. DOI: [10.1109/tdei.2019.007773](https://doi.org/10.1109/tdei.2019.007773).
4. Li H, Xie Z, Liu L, et al. High-performance insulation materials from poly(ether imide)/boron nitride nanosheets with enhanced DC breakdown strength and thermal stability. *IEEE Trans Dielectr Electr Insul* 2019; 26(3): 722–729. DOI: [10.1109/tdei.2018.007637](https://doi.org/10.1109/tdei.2018.007637).
5. Pandey JC and Singh M. Dielectric polymer nanocomposites: past advances and future prospects in electrical insulation perspective. *SPE Polym* 2021; 2: 236–256. DOI: [10.1002/PLS2.10059](https://doi.org/10.1002/PLS2.10059).
6. Keith Nelson J. *Dielectric Polymer Nanocomposites*. Springer, 2010. DOI: [10.1007/978-1-4419-1591-7](https://doi.org/10.1007/978-1-4419-1591-7). Dielectric Polymer Nanocomposites
7. Nazir MT, Shengtao BTP, Shakeel L, et al. Effect of micro - nano additives on breakdown , surface tracking and mechanical performance of ethylene propylene diene monomer for high voltage insulation. *J Mater Sci Mater Electron* 2019; 30(15): 14061–14071. DOI: [10.1007/s10854-019-01771-6](https://doi.org/10.1007/s10854-019-01771-6).
8. Rahim NH, Lau KY, Muhamad NA, et al. Structure and dielectric properties of polyethylene nanocomposites containing calcined zirconia. *IEEE Trans Dielectr Electr Insul* 2019; 26(5): 1541–1548. DOI: [10.1109/TDEL.2019.008149](https://doi.org/10.1109/TDEL.2019.008149).
9. Ayoob R, Alhabill F, Andritsch T, et al. Enhanced dielectric properties of polyethylene/hexagonal boron nitride nanocomposites. *J Mater Sci* 2018; 53(5): 3427–3442. DOI: [10.1007/s10853-017-1786-y](https://doi.org/10.1007/s10853-017-1786-y).
10. Tanaka T and Imai T. *Advanced Nanodielectrics: Fundamentals and Applications*. Florida, USA: CRC Press, 2017, <https://doi.org/10.1201/9781315230740>.
11. Pandey JC and Singh M. Evidences of interphase formation and concomitant change in the dielectric properties of epoxy-alumina nanocomposites. *Polym Test* 2020; 91: 106802. DOI: [10.1016/j.polymertesting.2020.106802](https://doi.org/10.1016/j.polymertesting.2020.106802).
12. Peng W, Rhim S, Zare Y, et al. Effect of “Z” factor for strength of interphase layers on the tensile strength of polymer nanocomposites. *Polym Compos* 2019; 40(3): 1117–1122. DOI: [10.1002/pc.24813](https://doi.org/10.1002/pc.24813).
13. Chen S, Sarafbidabad M, Zare Y, et al. Estimation of the tensile modulus of polymer carbon nanotube nanocomposites containing filler networks and interphase regions by development of the Kolarik model. *RSC Adv* 2018; 8(42): 23825–23834. DOI: [10.1039/c8ra01910j](https://doi.org/10.1039/c8ra01910j).
14. Zhou Z, Sarafbidabad M, Zare Y, et al. Prediction of storage modulus in solid-like poly (lactic acid)/poly (ethylene oxide)/carbon nanotubes nanocomposites assuming the contributions of nanoparticles and interphase regions in the networks. *J Mech Behav Biomed Mater* 2018; 86: 368–374. DOI: [10.1016/j.jmbbm.2018.06.044](https://doi.org/10.1016/j.jmbbm.2018.06.044).
15. Maity P, Basu S, Parameswaran V, et al. Degradation of polymer dielectrics with nanometric metal-oxide fillers due to surface discharges. *IEEE Trans Dielectr Electr Insul* 2008; 15(1): 52–61. DOI: [10.1109/T-DEL.2008.4446736](https://doi.org/10.1109/T-DEL.2008.4446736).
16. Raetzke S and Kindersberger J. Role of interphase on the resistance to high-voltage arcing, on tracking and erosion of silicone/SiO<sub>2</sub> nanocomposites. *IEEE Trans Dielectr Electr Insul* 2010; 17(2): 607–614. DOI: [10.1109/TDEL.2010.5448118](https://doi.org/10.1109/TDEL.2010.5448118).
17. Singh M, Rajendran VK and Pandey JC. A novel bisection method based algorithm to quantify interphase in epoxy alumina nanocomposites. *Comput Mater Sci* 2020; 183: 109912. DOI: [10.1016/j.commatsci.2020.109912](https://doi.org/10.1016/j.commatsci.2020.109912).
18. Zunjarrao SC and Singh RP. Characterization of the fracture behavior of epoxy reinforced with nanometer and micrometer sized aluminum particles. *Compos Sci Technol* 2006; 66(13): 2296–2305. DOI: [10.1016/j.compscitech.2005.12.001](https://doi.org/10.1016/j.compscitech.2005.12.001).
19. Ash BJ, Schadler LS and Siegel RW. Glass transition behavior of alumina/polymethylmethacrylate nanocomposites. *Mater Lett* 2002; 55(1–2): 83–87. DOI: [10.1016/S0167-577X\(01\)00626-7](https://doi.org/10.1016/S0167-577X(01)00626-7).
20. Rashidi V, Coyle EJ, Sebeck K, et al. Thermal conductance in cross-linked polymers: effects of non-bonding interactions. *J Phys Chem B* 2017; 121(17): 4600–4609. DOI: [10.1021/acs.jpcc.7b01377](https://doi.org/10.1021/acs.jpcc.7b01377).
21. Suleiman BM. Effective thermal conduction in composite materials. *Appl Phys A Mater Sci Process* 2010; 99(1): 223–228. DOI: [10.1007/s00339-009-5503-9](https://doi.org/10.1007/s00339-009-5503-9).
22. Andritsch T, Kochetov R, Morshuis PHF, et al. *Annual Report - Conference on Electrical Insulation and Dielectric Phenomena*. Denver, CO: CEIDP., 2011, pp. 624–627. DOI: [10.1109/CEIDP.2011.6232734](https://doi.org/10.1109/CEIDP.2011.6232734). Proposal of the polymer chain alignment model
23. Xu Y, Kraemer D, Song B, et al. Nanostructured polymer films with metal-like thermal conductivity. *Nat Commun* 2019; 10(1): 1–8. DOI: [10.1038/s41467-019-09697-7](https://doi.org/10.1038/s41467-019-09697-7).
24. Singh V, Bougher TL, Weathers A, et al. High thermal conductivity of chain-oriented amorphous polythiophene. *Nat Nanotechnol* 2014; 9(5): 384–390. DOI: [10.1038/nnano.2014.44](https://doi.org/10.1038/nnano.2014.44).

25. Shen S, Henry A, Tong J, et al. Polyethylene nanofibres with very high thermal conductivities. *Nat Nanotechnol* 2010; 5(4): 251–255. DOI: [10.1038/mnano.2010.27](https://doi.org/10.1038/mnano.2010.27).
26. Liu J and Yang R. Length-dependent thermal conductivity of single extended polymer chains. *Phys Rev B - Condens Matter Mater Phys* 2012; 86(10): 104307. DOI: [10.1103/PhysRevB.86.104307](https://doi.org/10.1103/PhysRevB.86.104307).
27. Lu C, Chiang SW, Du H, et al. Thermal conductivity of electrospinning chain-aligned polyethylene oxide (PEO). *Polymer (Guildf)* 2017; 115: 52–59. DOI: [10.1016/j.polymer.2017.02.024](https://doi.org/10.1016/j.polymer.2017.02.024).
28. Zhang T and Luo T. Role of chain morphology and stiffness in thermal conductivity of amorphous polymers. *J Phys Chem B* 2016; 120(4): 803–812. DOI: [10.1021/acs.jpcc.5b09955](https://doi.org/10.1021/acs.jpcc.5b09955).
29. Zhu B, Liu J, Wang T, et al. Novel polyethylene fibers of very high thermal conductivity enabled by amorphous restructuring. *ACS Omega* 2017; 2(7): 3931–3944. DOI: [10.1021/acsomega.7b00563](https://doi.org/10.1021/acsomega.7b00563).
30. Papkov D, Delpouve N, Delbreilh L, et al. Quantifying polymer chain orientation in strong and tough nanofibers with low crystallinity: toward next generation nanostructured superfibers. *ACS Nano* 2019; 13(5): 4893–4927. DOI: [10.1021/acsnano.8b08725](https://doi.org/10.1021/acsnano.8b08725).